Journal of Alloys and Compounds 505 (2010) 286–290

Contents lists available at ScienceDirect

Journal of Alloys and Compounds

journal homepage: www.elsevier.com/locate/jallcom

In-plane defects produced by ball-milling of expanded graphite

Xueqing Yue[a,b], Hua Wang[b], Shuying Wang[b], Fucheng Zhang[a], Ruijun Zhang[a,*]

[a] State Key Laboratory of Metastable Materials Science and Technology, Yanshan University, Qinhuangdao 066004, PR China
[b] Qinhuangdao Higher Vocational and Technical College, Qinhuangdao 066100, PR China

ARTICLE INFO

Article history:
Received 7 April 2010
Received in revised form 7 June 2010
Accepted 9 June 2010
Available online 18 June 2010

Keywords:
Expanded graphite
Ball-milling
Nanostructure evolution
Defects

ABSTRACT

Expanded graphite (EG) was ball-milled in a high-energy planetary-type mill under air atmosphere. The products were characterized by X-ray diffraction (XRD) and high resolution transmission electron microscopy (HRTEM). During the milling process (up to 100 h), the crystallite size (L_c) of EG decreases gradually from 15.4 to 11.3 nm. Compared with most of natural graphite, this L_c decrease degree of EG is far lower. In the EG after ball-milling for 100 h, plenty of in-plane defects are produced, which rarely occur in most of ball-milled natural graphite.

1. Introduction

In recent years carbon nanostructures have been received considerable attention of researchers for their unique properties, such as excellent electrical conductivity, high thermal resistance, low thermal expansion coefficient, and large surface area. Ball-milling has been proven to be one of the effective ways to produce carbon nanostructures. Extensive investigations were performed to characterize the nanostructures of ball-milled natural graphite [1–8], and generally ball-milling could produce various defects including delamination, translation, warping and curvature, as well as various carbon nanostructures including carbon nanoarches, closed-shells and tubes [9–12].

Expanded graphite (EG) is an important carbon material for the industrial production of flexible graphite sheets which are flexible, compactable and resilient. Usually EG is prepared by rapid heating of expandable graphite to a high temperature [13]. During the heating process of this solid, a huge unidirectional expansion of the initial graphite flakes occurs, and thus the characteristic porous structure of EG is formed. Graphene nanosheets formed by ball-milled EG could be used as adsorbent of 1,2-dichlorobenzene [14] and as conductive filler of Al_2O_3-based ceramic [15]. However, up to now, published work on the nanostructures of ball-milled EG is quite scarce.

In the present work, EG was ball-milled for 60, 80 and 100 h in a high-energy planetary-type mill under air atmosphere. We investigate the out-of plane crystallite size (L_c) evolution of EG during ball-milling by X-ray diffraction (XRD), as well as the defects produced in EG ball-milled for 100 h by high resolution transmission electron microscopy (HRTEM), and carry out a comparison with most of ball-milled natural graphite.

2. Experimental

2.1. Preparation of EG

At room temperature, 10 ml of concentrated sulphuric acid (98%) and 1 ml of hydrogen peroxide (30%) were mixed with 6 g of natural flake graphite (35 mesh, 99% purity, 97.5% crystallinity, purchased from Qingdao Tianhe Graphite Company, China). The mixture was placed for 90 min, washed with water to pH 5–7 and dried at 80 °C for 24 h, forming expandable graphite. EG (expanded volume of 250 ml/g) was prepared by heating the expandable graphite at 1000 °C for 15–20 s.

2.2. Ball-milling of EG

With a ball-to-EG weight ratio of 40:1, 2 g of EG powders and 80 g of GCr15 (52100) bearing steel balls (10 mm in diameter) were introduced to a vial. For preventing agglomeration of the powders, 180 ml of ethanol as milling medium was poured into the vial. Ball-milling was carried out for 60, 80 and 100 h in a GN-2 high-energy mill [16] (planetary-type, Shenyang New Electromechanical Equipment Factory, China) under air atmosphere with a rotation speed of 450 rpm.

2.3. Characterization

The nanostructure evolution of the samples was characterized by X-ray diffractometer (D/mx-rB, Rigaku, Japan) (Cu Kα, 40 kV, 100 mA, 10–90°, 0.02 step, 4° $step^{-1}$). Here the samples for XRD analysis were mounted in a plastic sample holder. Additional nanostructure information was obtained from HRTEM (JEOL-2010) set at 200 kV.

* Corresponding author. Tel.: +86 0335 8387462; fax: +86 0335 8064504.
E-mail address: yuexueqing@126.com (R. Zhang).

0925-8388/$ – see front matter © 2010 Elsevier B.V. All rights reserved.
doi:10.1016/j.jallcom.2010.06.048

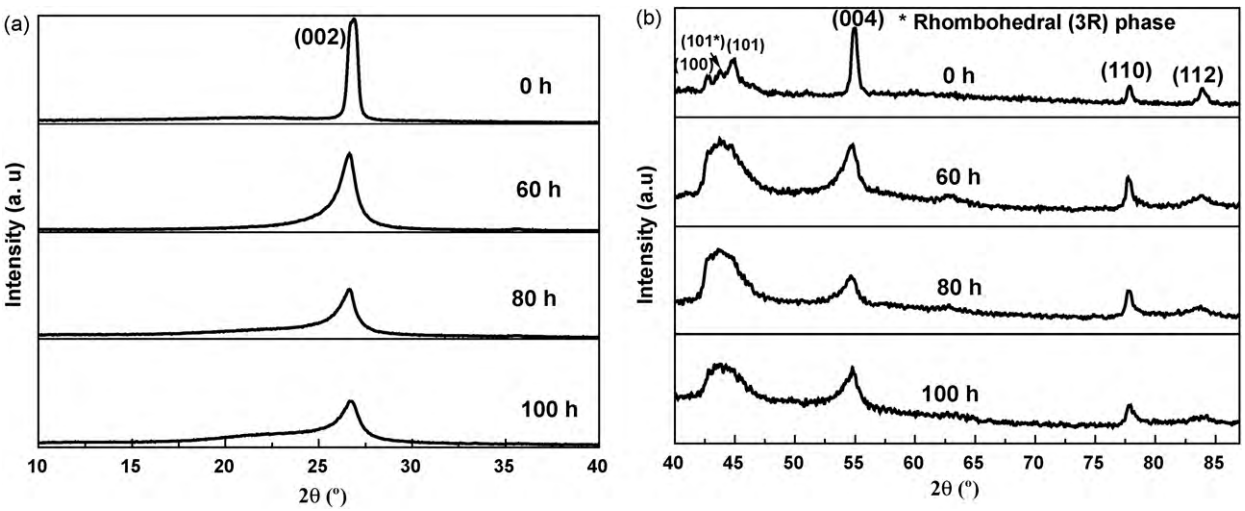

Fig. 1. XRD patterns of EG milled for 0, 60, 80 and 100 h: (a) (0 0 2) and (b) (1 0 0), (1 0 1*), (1 0 1), (0 0 4), (1 1 0) and (1 1 2) peaks.

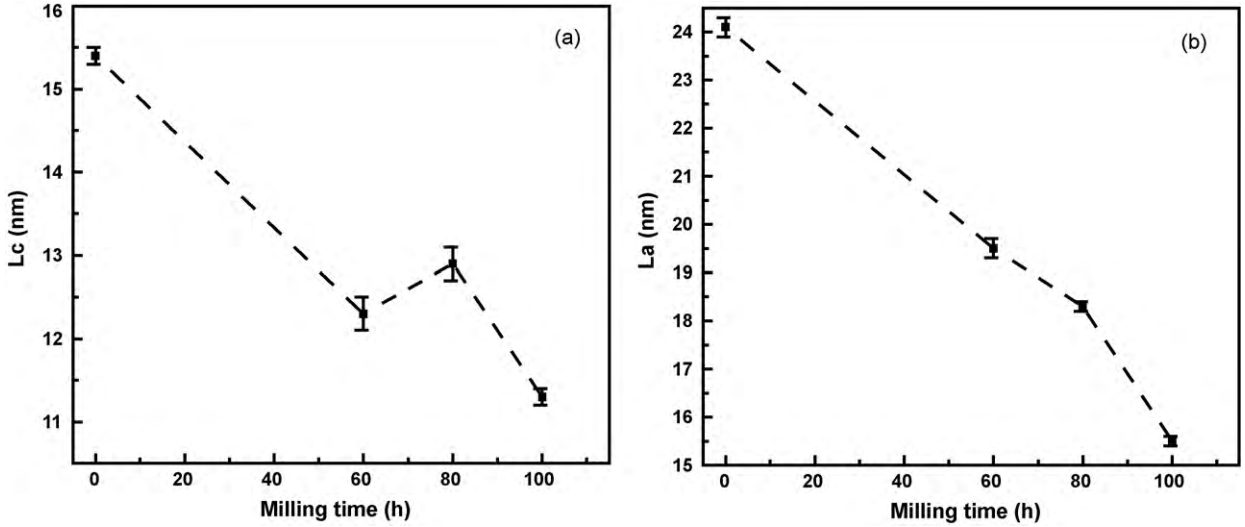

Fig. 2. Average L_c (a) and L_a (b) crystallite sizes of EG at various milling times.

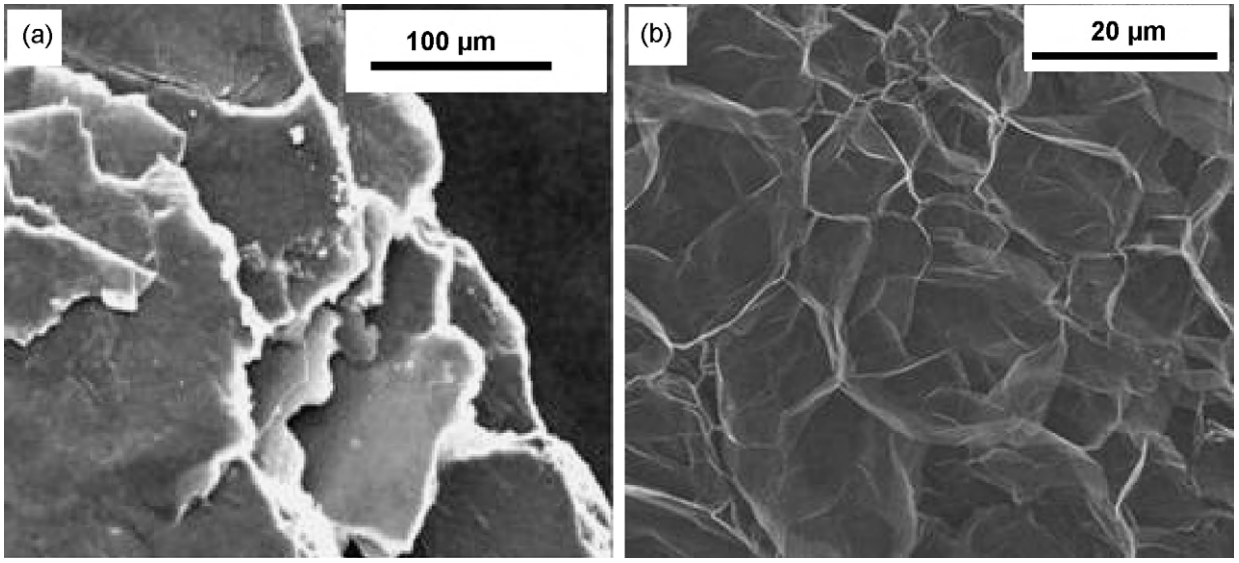

Fig. 3. SEM images of (a) natural graphite and (b) EG.

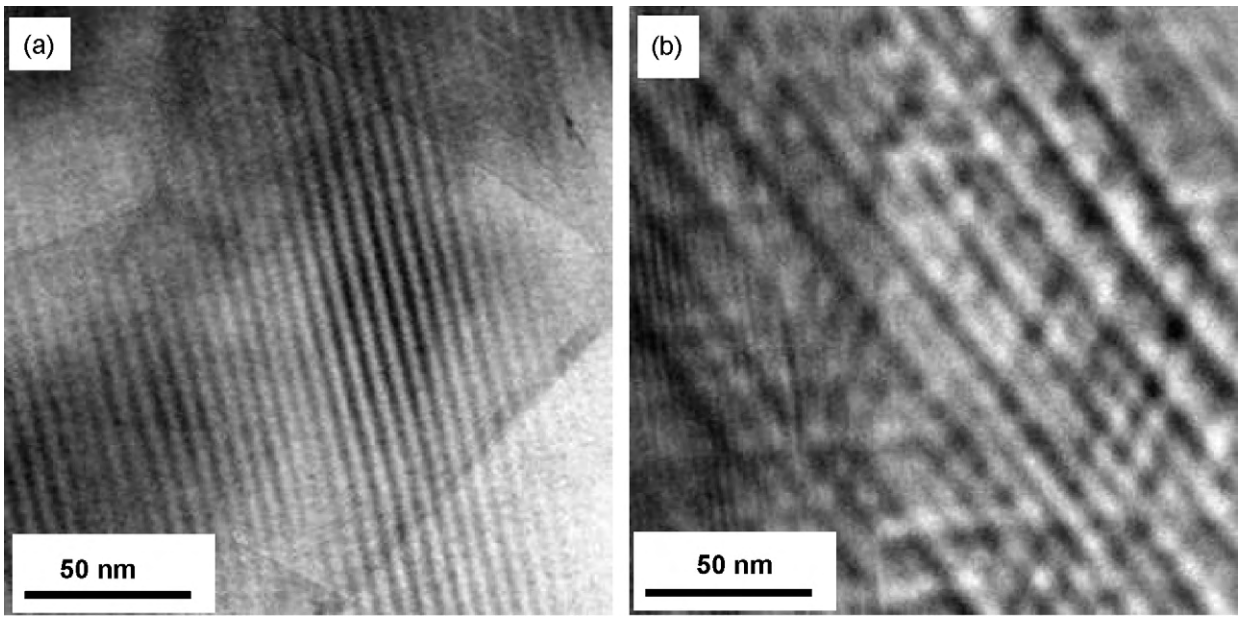

Fig. 4. TEM images of (a) natural graphite and (b) EG.

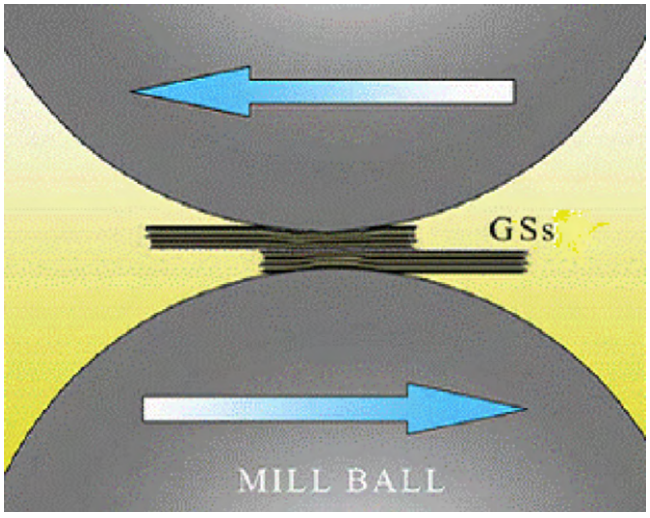

Fig. 5. Schematic illustration of cleavage of graphite sheets (GSs) from graphite pallets; the arrows indicate the shear effect during ball-milling.

3. Results and discussion

3.1. XRD analysis

Fig. 1 is the typical XRD patterns of EG at various milling times. It can be seen that the diffraction of the original EG is dominated by the super strong (0 0 2) peak. The (1 0 1*) peak at 43.7° is attributed to the rhombohedral phase of graphite which is present with the hexagonal phase. The main difference between the two phases relates to the stacking order of the graphene planes. It is ABABAB, . . . for the hexagonal phase and ABCABC, . . . for the rhombohedral phase [6]. During the milling process, the graphite peaks become broadened. After ball-milling for 60 h, the three peaks between 42° and 46° (1 0 0, 1 0 1* and 1 0 1) merge to a broad peak and become undistinguishable. It is noticed that the (1 1 2) peak is broadened more significantly compared with the (1 1 0) peak, which suggests that the (*h k l*) peak is more easily destroyed than the (*h k* 0) peak. This result is consistent with the established conclusion that the three-dimensional (3D) orders of crystalline graphite powders are easily destroyed during ball-milling [4,6].

With increasing the milling time, the (0 0 2) peak is shifted toward lower angles gradually, suggesting the widening of the d_{002} spacing caused by the destruction of the structure as well as

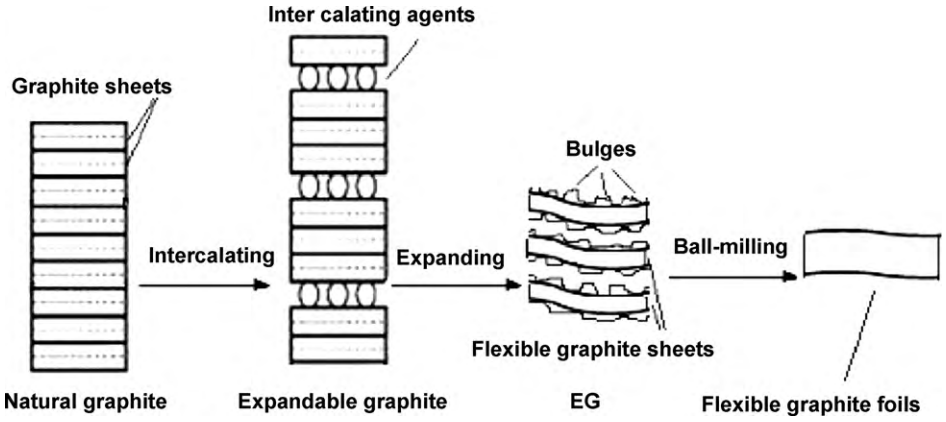

Fig. 6. Schematic illustration of structural evolution of natural graphite during intercalating, expanding and ball-milling.

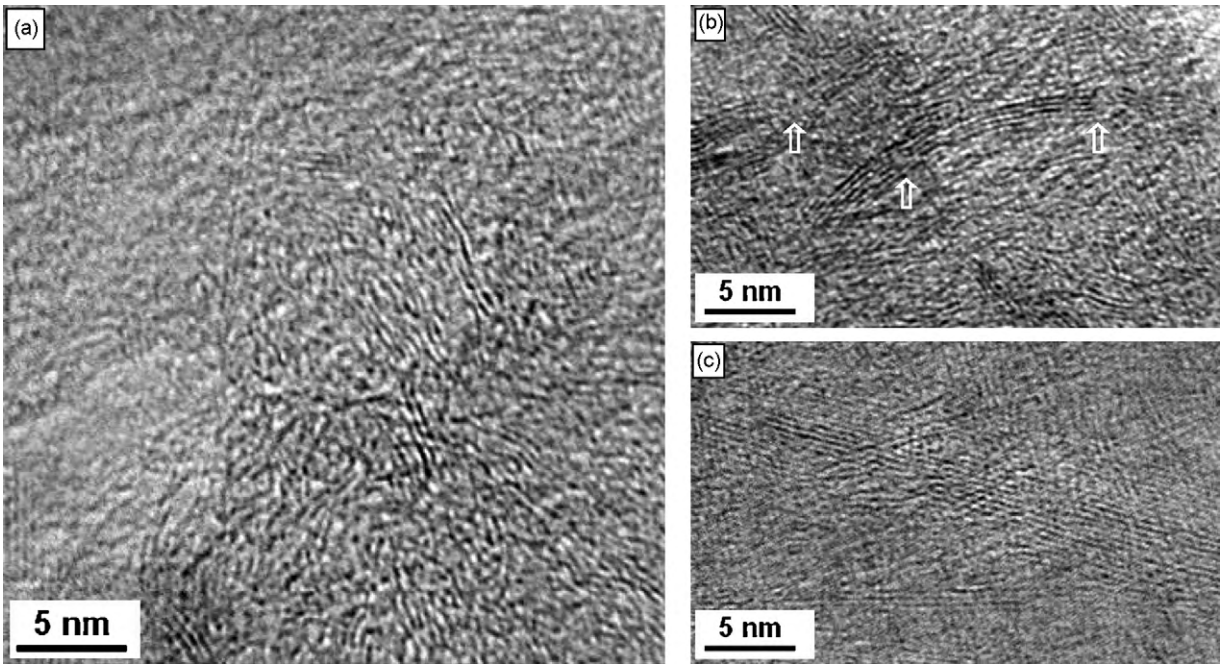

Fig. 7. HRTEM images of EG ball-milled for 100 h.

the generation of defects [17]. The asymmetric broadening of the (0 0 2) peak may relate to the reduction in the crystallite size, or the introduction of disordered graphene planes [11].

Fig. 2a and b shows the evolution of the average out-of plane (L_c) and in-plane (L_a) crystallite sizes of EG during ball-milling, respectively. The L_c and L_a reported are calculated from the (0 0 2) and (1 1 0) peaks, respectively, by using the Scherrer equation with corrections for the line broadening. After ball-milling for 100 h, the L_c decreases from 15.4 to 11.3 nm, while the L_a decreases from 24.1 to 15.5 nm. Compared with most of natural graphite [4,6,8], this L_c decrease degree of EG is far lower, which can be due to two factors, the structural difference of EG and natural graphite as well as the mechanism of planetary-type mill. During the intense and sudden heating process of expandable graphite, the natural graphite sheets are expanded due to the disjoining pressure created by water and SO_x, and the planar graphite sheets of natural graphite change to the crinkled paper shape of EG, as shown in Fig. 3. Their structural difference is also confirmed by the TEM images (Fig. 4). Fig. 4a exhibits the planar graphite sheets with uniform thickness of natural graphite, while Fig. 4b shows the expanded graphite sheets with bulges of EG. It is well known that the planetary-type mill favors the cleavage of the graphite sheets because the shear component of the applied stress is dominant, as shown in Fig. 5 [15]. For natural graphite, planetary ball mill is an effective method for the cleavage of the graphite sheets. However, the graphite sheets with crinkles of EG will be adhered together during the impact of the steel balls, forming flexible graphite foils with superior anti-stripping performance [18,19], as shown in Fig. 6. Therefore, the cleavage of the graphite sheets of EG becomes difficult, resulting in the lower decrease in the L_c.

3.2. HRTEM Investigations

Fig. 7 is the typical HRTEM images of the EG ball-milled for 100 h. From Fig. 7a, highly warped graphene planes can be frequently observed. The interplanar spacing increases up to 0.70 nm, which is a massive increase on the raw EG (0.335 nm). In addition, we can see some broken single-layer graphite sheets, forming in-plane vacancies. Fig. 7b exhibits two carbon nanoarches with bending angles of about 15° and nearly 180°, respectively, which should be caused by the direct curve of the graphite sheets. In the two carbon nanoarches, it can be seen several vacancies with width of 1–2 nm (white arrows) crossing the whole graphite sheets with thickness of 2 nm. Here plenty of broken single-layer graphite sheets are also observed. In addition, Fig. 7c shows stacking faults as well as plenty of in-plane vacancies. It should be pointed out that these defects do not derive from the raw EG, because its HMTEM exhibits that the planar graphene layers are maintained though a few planes are delaminated as the result of expansion.

For ball-milled graphite materials, the formation of carbon nanoarches should be due to the large bond strength difference between the in-plane very strong C–C bonds that constitute the hexagonal graphene planes and the weak out-of-plane π–π forces that hold these planes together. Preferential cleavage occurs along the weak interplanar bonds, but not the strong C–C network. Usually in-plane defects rarely occur. However, the crinkled graphite sheets of EG will often undergo folding during ball-milling, and the folded sheets are not easy to break due to the superior flexibility. As a consequence, the in-plane defects are produced and remained in ball-milled EG. On the other hand, the folded graphite sheets of natural graphite will often be broken, and thus in-plane defects are not easy to observe.

4. Conclusion

We investigate the nanostructure evolution of EG during high-energy ball-milling by XRD and HRTEM. Compared with most of natural graphite, the L_c decrease degree of EG is far lower during ball-milling. Ball-milling of EG not only produces highly warped graphene planes, carbon nanoarches and stacking faults, but also produces plenty of in-plane defects which rarely occur in most of ball-milled natural graphite.

References

[1] Y.A. Kim, T. Hayashi, Y. Fukai, M. Endo, T. Yanagisawa, M.S. Dresselhaus, Chem. Phys. Lett. 355 (2002) 279–284.
[2] T. Fukunaga, K. Nagano, U. Mizutani, H. Wakayama, Y. Fukushima, J. Non-Cryst. Solids 232–234 (1998) 416–420.

[3] T.D. Shen, W.Q. Ge, K.Y. Wang, M.X. Quan, J.T. Wang, W.D. Wei, et al., Nanostruct. Mater. 7 (1996) 393–399.
[4] M.V. Antisari, A. Montone, N. Jovic, E. Piscopiello, C. Alvani, L. Pilloni, Scripta Mater. 55 (2006) 1047–1050.
[5] R. Janot, D. Guerard, Carbon 40 (2002) 2887–2896.
[6] T.S. Ong, H. Yang, Carbon 38 (2000) 2077–2085.
[7] A. Touzik, M. Hentsche, R. Wenzel, H. Hermann, J. Alloys Compd. 21 (2006) 141–145.
[8] A. Mileva, M. Wilson, G.S.K. Kannangara, N. Tran, Mater. Chem. Phys. 111 (2008) 346–350.
[9] N.J. Welham, V. Berbenni, P.G. Chapman, J. Alloys Compd. 349 (2003) 255–263.
[10] X.H. Chen, H.S. Yang, G.T. Wu, M. Wang, F.M. Deng, X.B. Zhang, et al., J. Cryst. Growth 218 (2000) 57–61.
[11] J.Y. Huang, Acta Mater. 47 (1999) 1801–1808.
[12] J.L. Li, L.J. Wang, G.Z. Bai, W. Jiang, Scripta Mater. 54 (2006) 93–97.
[13] G.H. Chen, D.J. Wu, W.G. Weng, C.L. Wu, Carbon 41 (2003) 579–625.
[14] X.L. Li, G.H. Chen, Mater. Lett. 63 (2009) 930–932.
[15] Y.C. Fan, L.J. Wang, J.L. Li, J.Q. Li, S.K. Sun, F. Chen, L.D. Chen, W. Jiang, Carbon 48 (2010) 1743–1749.
[16] J.L. Li, F. Li, K. Hu, Y. Zhou, J. Alloys Compd. 334 (2002) 253–260.
[17] M. Francke, H. Hermann, R. Wenzel, G. Seifert, K. Wetzig, Carbon 43 (2005) 1204–1212.
[18] M.B. Dowell, R.A. Howard, Carbon 3 (1986) 311–323.
[19] R.A. Reynolds III, R.A. Greinke, Carbon 39 (2001) 473–481.